Farhad Namdari[1], Moslem Salehi[1*],

J. Electrical Systems 12-2 (2016): 373-386

Regular paper

Journal of Electrical Systems

Fault Classification and Location in Transmission Lines Using Traveling Waves Modal Components and Continuous Wavelet Transform (CWT)

Accurate fault classification and localization are the bases of protection for transmission systems. This paper presents a new method for classifying and showing location of faults by travelling waves and modal analysis. In the proposed method, characteristics of different faults are investigated using Clarke transformation and initial current traveling wave; then, appropriate indices are introduced to identify different types of faults. Continuous wavelet transform (CWT) is employed to extract information of current and voltage travelling waves. Fault location and classification algorithm is being designed according to wavelet transform coefficients relating to current and voltage modal components. The performance of the proposed method is tested for different fault conditions (different fault distance, different fault resistances, and different fault inception angles) by using PSCAD and MATLAB with satisfactory results.

Keywords: Fault classification, fault location, continuous wavelet transform, traveling wave, clark transform.

Article history: Received 6 January 2015, Accepted 15 April 2016.

1. Introduction

Fast and accurate detection, classification, and location of faults along power transmission and distribution networks can effetely improve power system reliability and performance, and also decrease operation costs [1], [2]. Recently, the travelling-wave-based fault location methods have many advantages such as high accuracy, reliability, stability and so, they are widely used in the power system [3]. The travelling wave fault location methods for transmission lines can generally be categorized into single- end, double-end and multi-end methods depending on the type of available measurements. In single-end methods, data from only one terminal of the transmission line are available and it does not need time synchronization or a communication link [4-7]. Double-end methods need measurements at both ends of the transmission line and a communication link [8-12]. In these methods, fault location can be calculated by comparing the arrival time of initial traveling waves at tow terminal of transmission line and the known propagation speed of the traveling wave. Multi-end methods that employ communication devices from the ends of the multiterminal transmission lines [13-17].

Traveling-wave-based techniques [18-23] extract transient signals generated by the fault and determine the location of fault. They are based on the relationship between forward- and backward-traveling waves which propagate along the transmission lines with a velocity close to the speed of light, and determination of the arrival times of the waves at transmission-line terminals. Wavelet transform (WT) is an effective method to detect the singularity and determining the arrival time of the traveling wave. The use of discrete

* Corresponding author: M. Salehi, Faculty of Engineering, Lorestan University,5th Km, Khorramabad, Tehran Hwy,P.O.Box:465, Khorramabad, Lorestan, Iran, E-mail: salehi.mo@fe.lu.ac.ir

[1] Faculty of Engineering, Lorestan University, Khorramabad, Lorestan, Iran.

wavelet transform (DWT) of modal components of the traveling waves initiated by faults is first proposed in [20], in order to determine the fault location. Also, this fault - location technique is applied to the teed circuits in [21]. Fault classification and faulty phase identification have an important role in protection of a transmission line. In [24], a technique based on fault-generated high-frequency signals and neural network was proposed for faulty phase identification. WT was used in [25] and [26] to extract the characteristics of the transient signals and wavelet coefficients are used for fault classification of a series-compensated transmission line. In other methods [27], [28], the artificial intelligent (AI) and fuzzy-logic techniques have been also presented for fault classification and faulted-phase selection. An algorithm of fault classification and faulted phase selection based on the initial current traveling wave was presented in [29]. Reference [30], has proposed traveling wave based fault location method in transmission lines using support vector machines (SVM) and neural network. A traveling-wave-based method for fault classification and localization for three-terminal circuits using machine learning was proposed in [31].

This paper presents a fault classification and localization method based on traveling waves for a transmission system using continuous wavelet transform (CWT) and Clark transform. The characteristics of various faults are investigated on the basis of the Clark transform and appropriate indices are introduced to identify different types of faults. Wavelet transform based on daubechies-4 (Db4) wavelet is adopted to extract the traveling wave from the postfault signals and to construct the algorithms.

2. Continuous Wavelet Transform and Wavelet Modulus Maxima

Wavelet Transform (WT) is a mathematical tool for signal analysis, and it has excellent ability of time – frequency localization. This proves to be advantageous in determining the wave-front of the initial travelling wave and the subsequent reflections. Given a function x (t), its continuous wavelet transform (CWT) will be calculated as [32]:

$$CWT_{(a,b)} = \frac{1}{\sqrt{|a|}} \int_{-\infty}^{+\infty} x(t)\, \phi^{*}(\frac{t-b}{a}) dt \tag{1}$$

where, a and b are the scaling (dilation) and translation (time shift) constants respectively, (t) is the mother wavelet, and '$*$' denotes a complex conjugate. Most of the information in a signal is carried by its irregular structures and its transient phenomena, called singularities. The modulus maxima of wavelet transforms are defined as the local maxima of the wavelet transforms if they satisfy the following conditions:

$$\forall \varepsilon > 0,\ \exists |t - t_0| < \varepsilon\ , t \neq t_0$$

$$\left|W(2^j, t_0)\right| < \left|W(2^j, t)\right| \tag{2}$$

Based on the above wavelet coefficients, the modulus maxima point of the wavelet transform coefficient (WTC) corresponds to the singularity of the signal. The mutation strength and direction in the signal can be identified by the amplitude and polarity of modulus maxima, respectively. Therefore the singularity of the traveling wave component

of post-fault current and voltage is equivalent to the modulus maxima of the wavelet transform. When the traveling wave arrives at the relay in transmission lines, the modulus maxima of the current and voltage wavelet transform appear accordingly.

3. Proposed method for fault classification and location

3.1. Phase to modal transform

Three phase lines have significant electromagnetic coupling between conductors. In order to implement the traveling wave method in three phase systems, the coupled voltages and currents are first decomposed into their modal components by means of the modal transformation matrices. Clarke's matrix is used as one of several common modal transformation matrices [20]:

$$\begin{bmatrix} M_0 \\ M_\alpha \\ M_\beta \end{bmatrix} = \frac{1}{3}\begin{bmatrix} 1 & 1 & 1 \\ 2 & -1 & -1 \\ 0 & \sqrt{3} & -\sqrt{3} \end{bmatrix}\begin{bmatrix} a \\ b \\ c \end{bmatrix} \tag{3}$$

where a, b, c represent the voltage or current values of the phase A, B, C respectively; M_0, M_α, M_β represent the modal values. Recorded phase signals are first transformed into their modal components. M_0 is the ground mode component, and its magnitude is significant only during faults having a path to ground. M_α, M_β are the decoupled aerial modes. Such simple transformations are real and can be used with any transposed line.

3.2. Fault characterization under the Clarke transform and fault detection criteria

In this section the characteristics of various faults are investigated on the basis of the Clark transform and the criteria of fault classification and faulted-phase selection are specified.

Single-Phase Grounding Fault: Fig. 1 shows the simplified diagram of single-phase grounding fault (AG). Assuming the grounding resistance is zero, the instantaneous boundary conditions at fault point are

$$\begin{aligned} i_B &= i_C = 0 \\ v_A &= 0 \end{aligned} \tag{4}$$

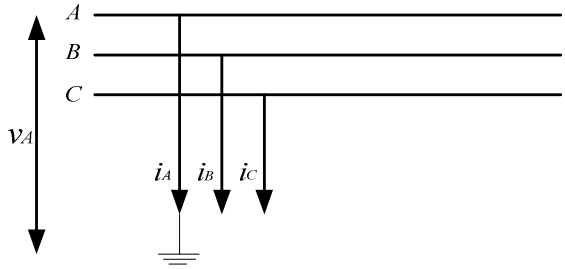

Fig.1. Single-phase grounding fault (AG).

According to (3), the instantaneous modal components can be obtained as

$$\begin{cases} M_0 = \frac{1}{3} i_A \\ M_\alpha = \frac{2}{3} i_A \\ M_\beta = 0 \end{cases} \quad (5)$$

Phase-to-Phase Fault: Fig. 2 shows the simplified diagram of the phase-to-phase fault (AB). Assuming the fault resistance is zero, the instantaneous boundary conditions at fault point are

$$\begin{cases} i_A = -i_B \\ i_C = 0 \\ v_A = v_B \end{cases} \quad (6)$$

And the modal components are obtained as follows:

$$\begin{cases} M_0 = 0 \\ M_\alpha = i_A \\ M_\beta = -\sqrt{3}\, i_A \end{cases} \quad (7)$$

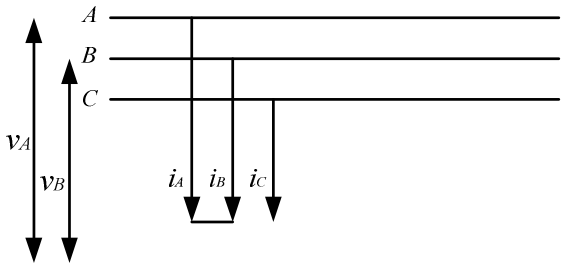

Fig.2. Phase-to-phase fault (AB).

Table1 : Characteristics of various fault in different situations and their detection criteria

Fault	M_0	M_α	M_β	detection criteria
AG	$\frac{1}{3} i_A$	$\frac{2}{3} i_A$	0	$M_\beta = 0$
BG	$\frac{1}{3} i_B$	$-i_B$	$\sqrt{3} i_B$	$\lvert M_\beta \rvert = \sqrt{3} \lvert M_\alpha \rvert$ & $P(M_\beta) \neq P(M_\alpha)$
CG	$\frac{1}{3} i_C$	$-i_C$	$-\sqrt{3} i_C$	$\lvert M_\beta \rvert = \sqrt{3} \lvert M_\alpha \rvert$ & $P(M_\beta) = P(M_\alpha)$
AB	0	i_A	$-\sqrt{3} i_A$	$M_0 = 0$ & $\lvert M_\alpha \rvert = \sqrt{3} \lvert M_\beta \rvert$ & $P(M_\beta) \neq P(M_\alpha)$
AC	0	i_A	$\sqrt{3} i_A$	$M_0 = 0$ & $\lvert M_\alpha \rvert = \sqrt{3} \lvert M_\beta \rvert$ & $P(M_\beta) = P(M_\alpha)$
BC	0	0	$2\frac{\sqrt{3}}{3} i_B$	$M_0 = 0$ & $M_\alpha = 0$
ABG	$\frac{1}{3}(i_A + i_B)$	$\frac{1}{3}(2i_A - i_B)$	$\frac{\sqrt{3}}{3} i_B$	$\lvert 2M_0 - M_\alpha \rvert = \sqrt{3} \lvert M_\beta \rvert$ & $P(2M_0 - M_\alpha) = P(\sqrt{3} \lvert M_\beta \rvert)$
ACG	$\frac{1}{3}(i_A + i_C)$	$\frac{1}{3}(2i_A - i_C)$	$-\frac{\sqrt{3}}{3} i_C$	$\lvert 2M_0 - M_\alpha \rvert = \sqrt{3} \lvert M_\beta \rvert$ & $P(2M_0 - M_\alpha) \neq P(\sqrt{3} M_\beta)$
BCG	$\frac{1}{3}(i_B + i_C)$	$-\frac{1}{3}(i_B + i_C)$	$\frac{\sqrt{3}}{3}(i_B - i_C)$	$\lvert M_0 \rvert = \lvert M_\alpha \rvert$ & $P(M_0) \neq P(M_\alpha)$
ABC(G)	0	$-(i_B + i_C)$	$\frac{\sqrt{3}}{3}(i_B - i_C)$	$M_0 = 0$ & No phase to phase fault

According to the above analyses, other faults were also investigated. Characteristics of various faults and their detection criteria in all possible situations are shown in Table 1. In Table 1, P indicates polarity. For example, when the equations $|M_\beta| = \sqrt{3}|M_\alpha|$ are satisfied and the polarity of M_α should be the same as that of M_β, it can be decided that single phase to ground fault (CG) occurs.

3.3. Fault location proposed algorithm

In this section, the proposed method is described for fault location based on voltage travelling waves and CWT. Lattice diagram [20] for two faults located at F1 and F2 is demonstrated in Figure 3. First, it is assumed that, if a ground fault occurs in the first half of transmission line at F1 and the primary travelling wave at t_{11} and its reflected wave from the fault point at t_{12} reach bus A, then the distance of fault point from bus A can be calculated as:

$$x = \frac{v_\alpha \Delta t}{2}$$
$$\Delta t = t_{12} - t_{11} \quad (12)$$

where v_α is velocity of voltage travelling wave of mode α. If a fault is assumed to occur in the second half of the transmission line at F_2 and the primary travelling wave at t_{21} and the wave reflected from bus B reach bus A at t_{22}, the distance of fault point from bus A is calculated as:

$$x = L - \frac{v_\alpha \Delta t}{2}$$
$$\Delta t = t_{22} - t_{21} \quad (13)$$

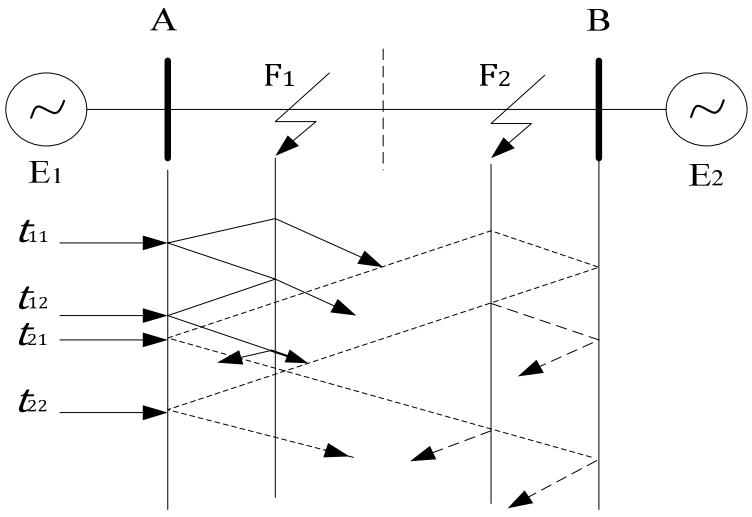

Fig.3. Lattice diagram for faults at F1 and F2

where L is length of total transmission line and v_α is velocity of voltage travelling wave in mode α. The important point in fault calculation is that, before applying equations (12) and (13), it should be recognized whether fault occurs in the first or second halves of the transmission line. In [20], this problem was solved using DWT at scale 1. In this paper, the

above problem is solved considering the polarity of CWT coefficients; thus, if the polarity of the first and second peaks of wavelet transform coefficients relating to mode α is equal,

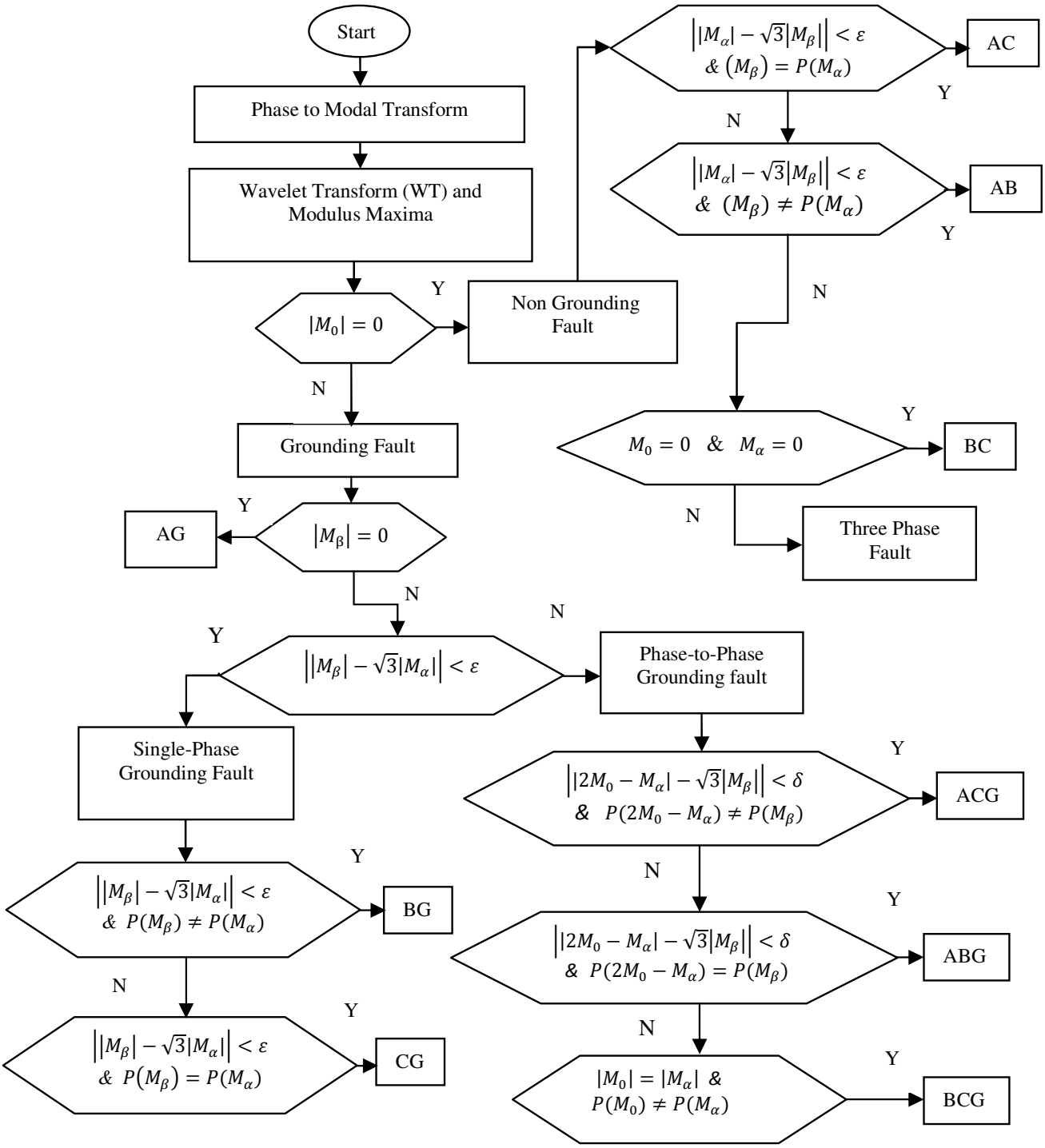

Fig.4. Flowchart of the proposed fault classification method

fault will occur in the second half of the transmission line; otherwise, it will occur in the first half. To summarize, steps of the proposed fault classification and localization algorithm are explained below:

Step 1: Transforming phase signals (voltage and current) into modal components by Clark transformation

Step 2: Applying CWT for modal components and calculating their modulus maxima
Step 3: Identifying fault type (ground or non-ground) using ground mode components (M_0)
Step 4: Investigating determined criteria for each fault and identifying fault type
Step 5: Identifying the half of transmission line in which fault occurs by the polarity of the first and second peaks of WTCs relating to mode α (for ground faults)
Step 6: Calculating fault distance by equations (12) and (13) for the faults occurring in the first and second halves of the transmission line, respectively. Since M_0 mode of non-ground faults is zero, equation (12) can be used for their distance calculation.

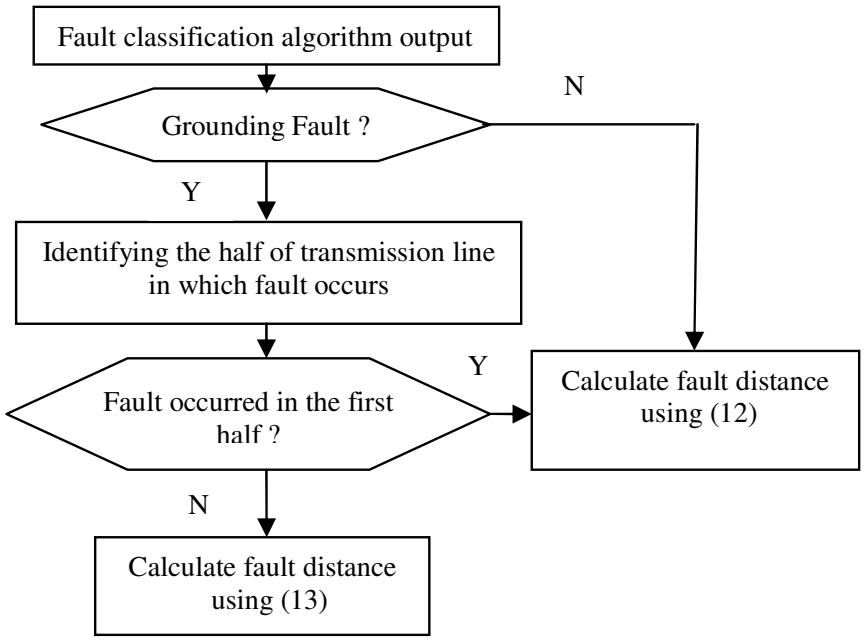

Fig.5. Flowchart of the proposed fault location method

Block diagrams of the proposed algorithm for classifying fault and determining faulty phase and for locating fault are depicted in Figures 4 and 5, respectively. In Figure 4, ε and δ are employed to consider measurement error and calculation error. For more reliability, ε and δ are considerhed 0.0001 and 0.1 in the present simulations, respectively.

4. Simulation results

To investigate performance of the proposed method for fault classification and location, a 500 kV, 60 Hz three-phase transmission system [32] with the structure depicted in Figure 3 is studied. The system data and parameters can be found in Appendix. All types of faults in different conditions and distances are considered. The MATLAB Wavelet Toolbox (db4 mother wavelet) has been used to implement the proposed method. The sampling frequency is set at 200 kHz. The propagation speed of traveling waves related to aerial mode (v_α) on the lines was 289.9 km/ms.

All types of faults including single-phase-to-ground, phase-to-phase fault, phase-to-phase grounding fault, and three phase fault are simulated for different system conditions. Tables 2 to 4 present the results relating to single-phase-to-ground fault, phase-to-phase fault, and phase-to-phase grounding fault. The fault resistance is 0.5 Ω, and the fault

inception angel is 35 degree. The results show that error percent is negligible for different fault distances and does not depend on the fault type; i.e. the proposed fault location has very good precision and is insensitive to fault type.

Table 2: Fault-type identification and fault location for different cases (single phase grounding fault)

Fault Type (Actual)	Actual fault distance (km)	M_α	M_β	M_0	Fault Type (Detected)	Calculated fault distance (km)	Error(%)
AG	90	-0.2121	0	-0.2921	AG	89.869	0.03
	160	-0.1425	0	-0.334	AG	160.169	0.04
	210	-0.2267	0	-0.2193	AG	210.177	0.029
	290	-0.2305	0	-0.3201	AG	289.838	0.045
BG	90	-0.08658	0.15	0.2383	BG	89.869	0.03
	160	-0.05808	0.1006	0.2728	BG	160.169	0.04
	210	-0.09251	0.1602	0.179	BG	210.177	0.029
	290	-0.09407	0.1629	0.2614	BG	289.838	0.045
CG	90	-0.01947	-0.03367	0.05375	CG	89.869	0.03
	160	-0.01316	-0.02279	0.06126	CG	160.169	0.04
	210	-0.02083	-0.03608	0.04033	CG	210.177	0.029
	290	-0.02119	-0.03607	0.05869	CG	289.838	0.045

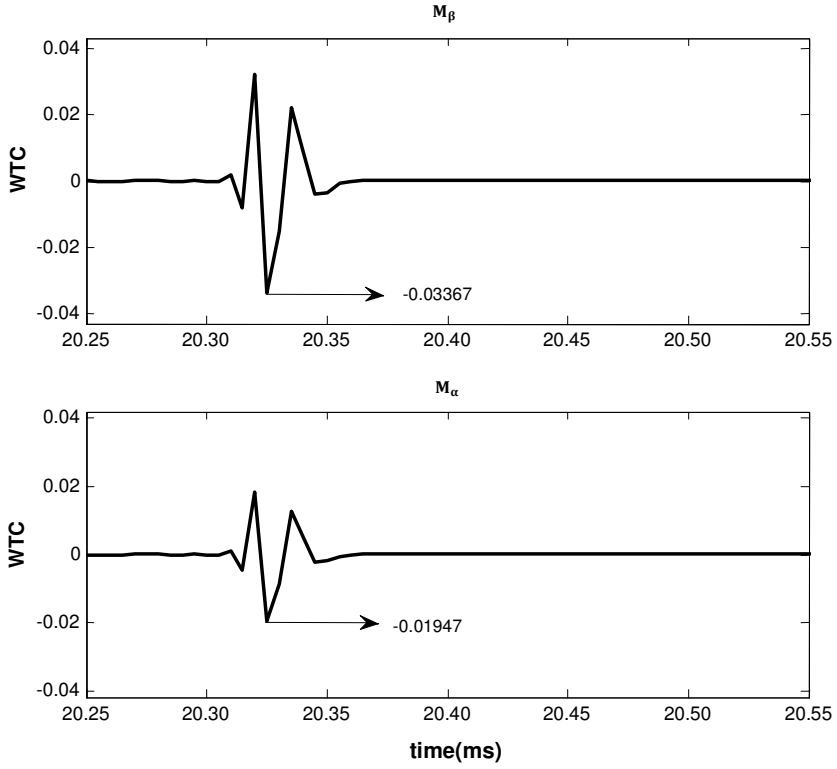

Fig.6. Current WTCs in α and β modes for single phase grounding fault (CG)

Figure 6 illustrates the simulation results of single-phase grounding fault (CG) at 60 km from bus A. In this figure, considering Current WTCs relating to M_α and M_β components, it is clear that these modes have equal polarity and :

$$M_\beta - \sqrt{3}M_\alpha = 0.1755 - \sqrt{3} \times 0.1013 = 4 \times 10^{-5} \cong 0$$

Therefore, the above results based on the criteria given in Table 1 reveal that single phase to ground fault CG occurs. Figure 7 shows voltage WTCs in α mode for single phase

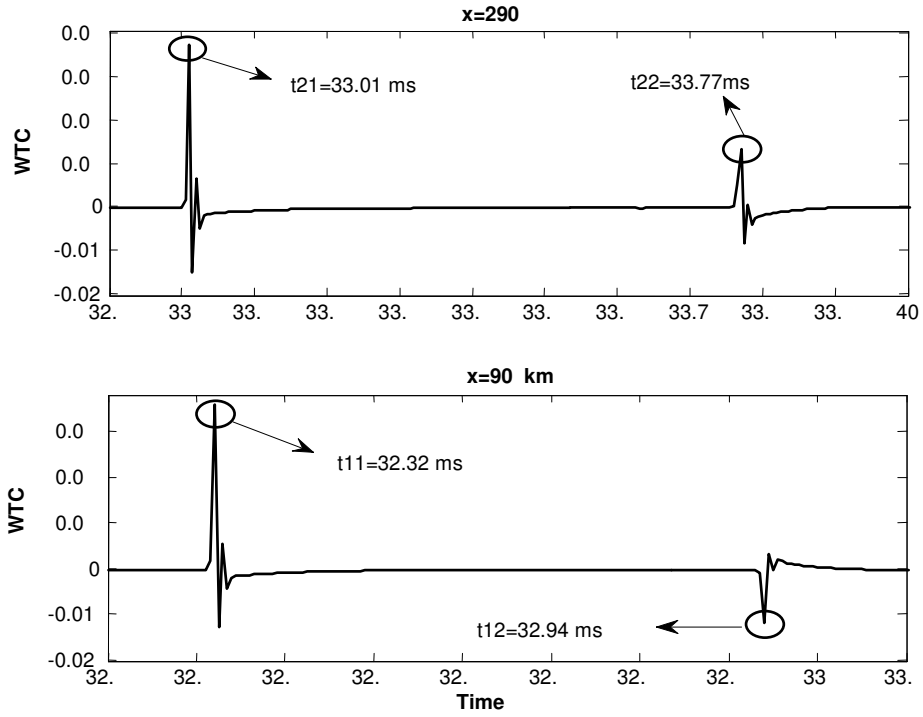

Fig.7. Voltage WTCs in mode α for single phase grounding fault (BG) at distance of 290 and 90 km from bus A

to ground fault (BG) in two cases. In the second case fault occurs at the distance of 90 km from bus A. According to Figure 7, polarity of the first and second coefficients is equal. Thus, fault occurs in the second half of the transmission line. Therefore, fault distance is calculated by equation (13) as follows:

$$x = 400 - \frac{289.9(33.77 - 33.01)}{2} = 289.838\ km$$

In the second case in which fault occurs at the distance of 90 km from bus A, polarity of coefficients is not equal. Fault distance can be also calculated by equation (12):

$$x = \frac{289.9(32.94 - 32.32)}{2} = 89.869\ km$$

To evaluate performance of the proposed method for fault locating, error percent is stated by the following equation:

$$\text{Error (\%)} = \frac{|\ \text{Calculated fault distance} - \text{Real distance distance}\ |}{\text{Length of total transmission line}} \times 100 \qquad (14)$$

Error percent for the above example in the first and second states is 0.045 and 0.03275, respectively. These results demonstrate very good precision of the proposed method in fault location.

Table 3: Fault-type identification and fault location for different cases (phase-to-phase grounding fault)

Fault Type (Actual)	Actual fault distance (km)	M_α	M_β	M_0	Fault Type (Detected)	Calculated fault distance (km)	Error (%)
AB	90	-0.4519	0.2609	0	A B	89.869	0.03
	160	-0.3078	0.1777	0	A B	160.169	0.04
	210	-0.4899	0.2829	0	A B	210.177	0.029
	290	-0.4982	0.2876	0	A B	289.9	0.155
BC	90	0	0.1814	0	BC	89.869	0.03
	160	0	0.1234	0	BC	160.169	0.04
	210	0	0.1970	0	BC	210.177	0.029
	290	0	0.2003	0	BC	289.838	0.045
AC	90	-0.2948	-0.1702	0	A C	89.869	0.03
	160	-0.2009	-0.1160	0	A C	160.169	0.04
	210	-0.3193	-0.1844	0	A C	210.177	0.029
	290	-0.3247	-0.1875	0	A C	289.838	0.045

Table 4: Fault-type identification and fault location for different cases (phase-to-phase fault)

Fault Type (Actual)	Actual fault distance (km)	M_α	M_β	M_0	Fault Type (Detected)	Calculated fault distance (km)	Error (%)
ABG	90	0.05061	-0.05077	-0.05364	ABG	89.869	0.03
	160	0.04507	-0.04516	-0.05751	ABG	160.169	0.04
	210	0.05489	-0.05506	-0.04594	ABG	210.177	0.029
	290	0.05399	-0.05416	-0.05488	ABG	289.9	0.155
BCG	90	0.0199	0.05402	-0.01945	BCG	89.869	0.03
	160	0.01771	0.04816	-0.01755	BCG	160.169	0.04
	210	0.02164	0.0587	-0.02137	BCG	210.177	0.029
	290	0.02132	0.05781	-0.02124	BCG	289.9	0.155
ACG	90	-0.05016	-0.05056	0.05381	ACG	89.869	0.03
	160	-0.0445	-0.04489	0.05765	ACG	160.169	0.04
	210	-0.05441	-0.05484	0.04608	ACG	210.177	0.029
	290	-0.05352	-0.05394	0.05502	ACG	289.9	0.155

4.1. Effect of fault resistance

A wide range of fault resistance values from 0.01 to 100 Ω is simulated to study the effect of fault resistance on the performance of the proposed method. Fault inception angel is adjusted at 30 degree. Table 5 presents some of the obtained results. According to the results, changes in fault resistance do not have any effect on the proposed method.

4.2. Effect of Fault Inception Angle

In this section, effect of fault inception angel on the proposed fault location and classification algorithm by simulating different cases is investigated. Results obtained from single-phase-to-ground fault (CG) at the distance of 30 km, phase-to-phase grounding fault (BCG) at 160 km, and phase-to-phase fault (AC) at 290 km from bus A with the fault

Table 5: Fault-type identification and fault location for different fault resistance

	Fault Resistance (Ω)	M_α	M_β	M_0	Fault Type (Detected)	Calculated fault distance (km)	Error(%)
AG at 160 km from bus A	0.01	-0.0143	0	-0.334	AG	160.169	0.04
	1	-0.01423	0	-0.3325	AG		
	5	-0.01397	0	-0.3265	AG		
	50	-0.116	0	-0.2711	AG		
	100	-0.09763	0	-0.2281	AG		
BC at 90 km from bus A	0.01	0	0.184	0	BC	89.869	0.03
	1	0	0.1827	0	BC		
	5	0	0.1775	0	BC		
	50	0	0.1345	0	BC		
	100	0	0.106	0	BC		

resistance of 5 Ω are presented in Table 6. According to the results, fault inception angel does not have any impact on the performance of the proposed algorithm.

Effect of fault inception angel is higher while passing through zero-crossing point. When the fault occurs at the zero-crossing point of one of phase voltages, a phase-to-phase grounding fault may be mistaken as a single-phase grounding fault. To study the above issue phase-to-phase grounding fault (ABG) and single-phase grounding fault (BG) are simulated at the distance of 90 km from bus A. In this simulation, the fault inception angle is set to simulate the zero-crossing point of phase A voltages. Figures 8 and 9 show WTCs related to current modal components (scale 2) in single-phase grounding fault (BG) and phase-to-phase grounding fault (ABG), respectively. Numerical results of both faults are presented in Table 7.

Table 6: Fault-type identification and fault location for different fault inception angle

	Fault Inception Angle (deg)	M_α	M_β	M_0	Fault Type (Detected)	Calculated fault distance (km)	Error(%)
CG at 30 km from bus A	0	-0.09212	-0.1596	0.3083	CG	29.714	0.07
	15	-0.09402	-0.1628	0.3146	CG		
	90	-0.05137	-0.08897	0.1721	CG		
AC at 290 km from bus A	35	-0.4567	-0.2637	0	AC	289.838	0.045
	110	0.07804	0.4504	0	AC		
	250	0.5015	0.2895	0	AC		
BCG at 160 km from bus A	10	0.01596	0.05704	-0.05538	BCG	160.169	0.04
	250	-0.01547	-0.07731	0.0537	BCG		
	350	0.01605	0.07214	-0.05569	BCG		

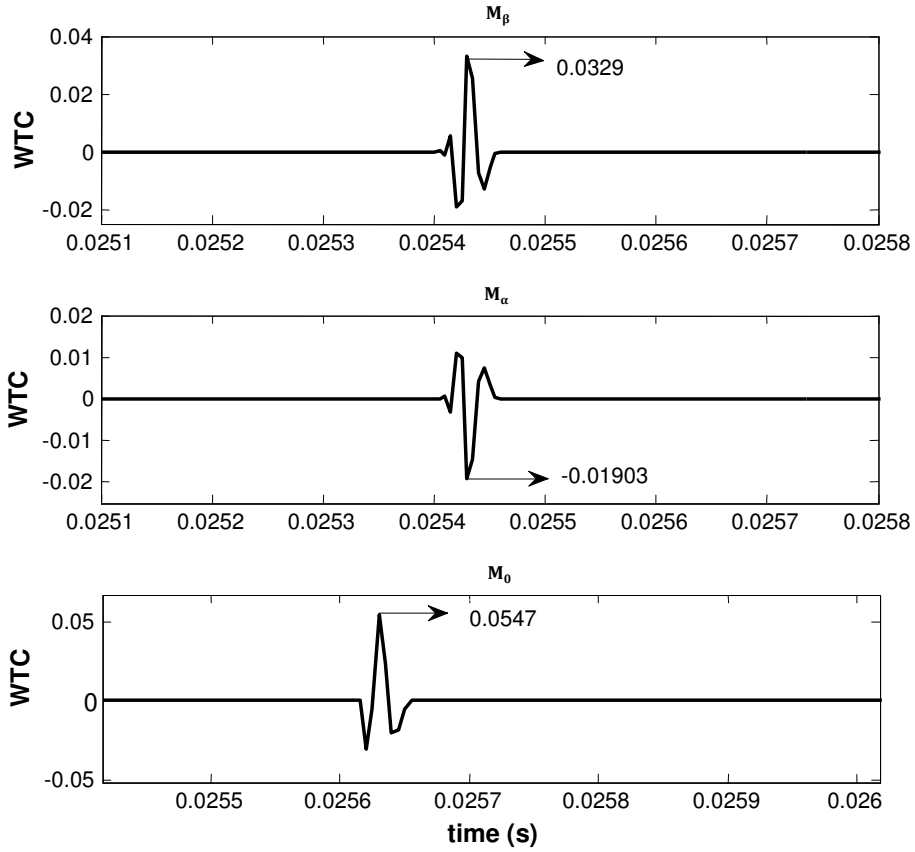

Fig.8. Current WTCs relating to M_0, M_α and, M_β for single phase to ground fault (BG)

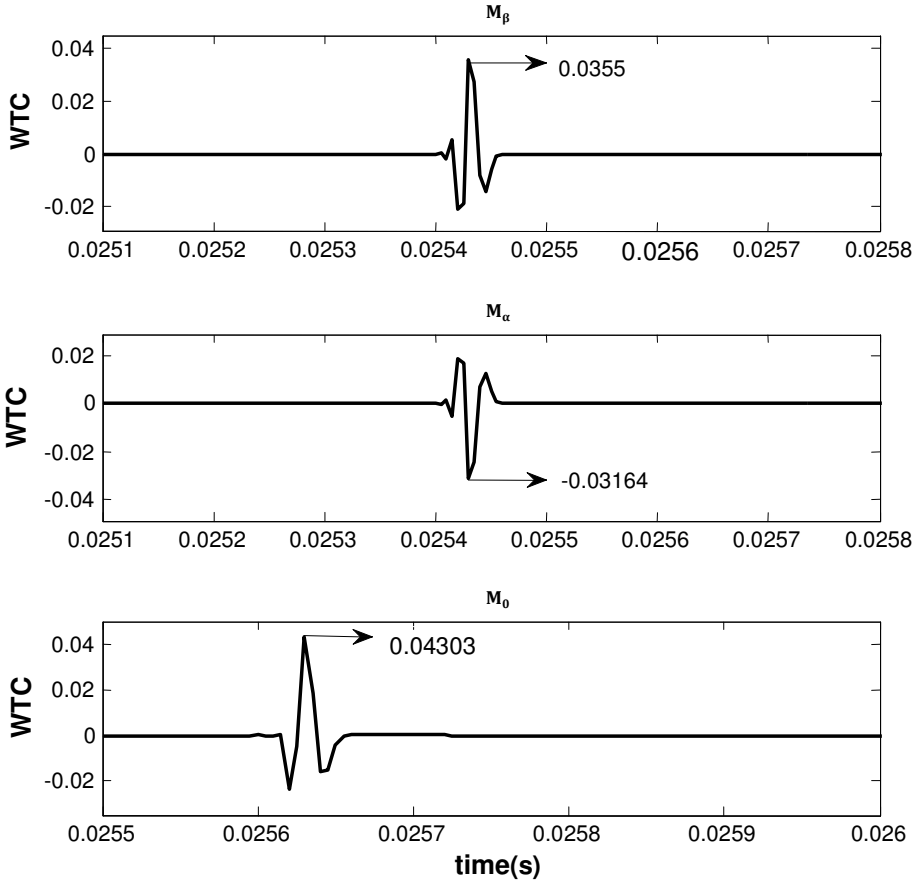

Fig.9. Current WTCs relating to M_0, M_α and, M_β for phase to phase to ground fault (ABG)

Table 7: Fault-type identification (Phase A voltage zero-crossing)

Fault Type (Actual)	M_α	M_β	M_0	Fault Type (Detected)
BG	-0.01903	0.03296	0.05476	BG
ABG	-0.03164	0.03555	0.04303	ABG

Given the results shown in Figures 8 and 9 and Table 7, the proposed fault location and classification method in a particular situation (Occurring fault at the zero-crossing point of one of phase voltages) precisely identifies the fault type.

5. Conclusion

In this paper, a method was proposed for fault location and classification based on travelling waves in transmission lines. In this method, first, phase signals are analyzed by Clark transformation into modal components. Wavelet transform coefficients (WTCs) of modal components were then calculated at the appropriate scale (1 and 2). Afterwards, appropriate indices are introduced to identify different types of faults based on amplitude and polarity of these coefficients and the proposed algorithm was designed for fault classification. Once the fault is classified, the wavelet coefficients of aerial-mode voltages are used to locate the fault. The performance of the proposed method is tested for various fault scenarios. Results show that the proposed method can precisely identify all fault types in different conditions, and determine the fault distance especially in phase-to-phase grounding fault situation with the zero-crossing point of one of the phase voltages. Furthermore, the presented method is not affected by fault distances, fault impedances, fault inception angles and fault types.

References

[1] X. Lin, H. Weng & B. Wang, A generalize method to improve the location accuracy of the single-ended sampled data and lumped parameter model based fault locators, *Int. J. Electr.Power Energy Syst*, 31(5), 201–205, 2009.

[2] D. Spoor & J.G.Zhu, Improved single-ended traveling-wave fault location algorithm based on experience with conventional substation transducers, *IEEE Trans. Power Deliv*, 23(3), pp. 1714–1720, 2006.

[3] P .Jafarian & M. Sanaye-Pasand, A traveling-wave-based protection technique using wavelet/PCA analysis, *IEEE Trans. Power Deliv*, 25(2), 588–599, 2010.

[4] T. Takagi, Y. Yamakoshi, M. Yamaura, R. Kondow & T. Matsushima, Development of a new type fault locator using the one-terminal voltage and current data, *IEEE Trans. Power App. Syst*, 101(8), 2892–2898, 1982.

[5] L. Eriksson, M. M. Saha & G. D. Rockefeller, "An accurate fault locator with compensation for apparent reactance in the fault resistance resulting from remore-end infeed," *IEEE Trans. Power App. Syst.*, 104(2), 423–436, 1985.

[6] T. Kawady & J. Stenzel, A practical fault location approach for double circuit transmission lines using single end data, *IEEE Trans.Power Del.*, 18(4), 1166–1173, 2003.

[7] C. E. M. Pereira & L. C. Zanetta, Jr., Fault location in transmission lines using one-terminal postfault voltage data, *IEEE Trans. Power Del.*, 19(2), 570–575, 2004.

[8] M. Kezunovic & B. Perunicic, Automated transmission line fault analysis using synchronized sampling at two ends, *IEEE Trans. Power Syst.*, 11(1), 441–447, 1996.

[9] A. L. Dalcastagnê, S. N. Filho, H. H. Zürn, & R. Seara, An biterative two-terminal fault-location method based on unsynchronized phasors, *IEEE Trans. Power Del.*, 23(4), 2318–2329, 2008.

[10] Y. Liao & N. Kang, Fault-location algorithms without utilizing line parameters based on the distributed parameter line model, *IEEE Trans.Power Del.*, 24(2), 579–584, 2009.

[11] J. Izykowski, E. Rosolowski, P. Balcerek, M. Fulczyk, & M. M. Saha, Accurate noniterative fault location algorithm utilizing two-end unsynchronized measurements, *IEEE Trans. Power Del*., 25(1), 72–80, 2010.

[12] C. A. Apostolopoulos & G. N. Korres, A novel algorithm for locating faults on transposed/untransposed transmission lines without utilizing line parameters, *IEEE Trans. Power Del.*, 25(4), 2328–2338, 2010.
[13] T. Nagasawa, M. Abe, N. Otsuzuki, T. Emura, Y. Jikihara, & M. Takeuchi, Development of a new fault location algorithm for multiterminal two parallel transmission lines, *IEEE Trans. Power Del.*, 7(3), 1516–1532, 1992.
[14] D. A. Tziouvaras, J. B. Roberts, & G. Benmouyal, New multi-ended fault location design for two- or three-terminal lines, in *Proc. 7th Int.Conf. Develop. Power Syst. Protection*, pp. 395–398, 2001.
[15] G. Manassero, E. C. Senger, R. M. Nakagomi, E. L. Pellini, & E. C. N. Rodrigues, Fault-location system for multiterminal transmission lines, *IEEE Trans. Power Del.*, 25(3), 1418–1426, Jul. 2010.
[16] T. Funabashi, H. Otoguro, Y. Mizuma, L. Dube, & A. Ametani, Digital fault location for parallel double-circuit multi-terminal transmission lines, *IEEE Trans. Power Del*., 15(2), 531–537, 2000.
[17] S. M. Brahma, Fault location scheme for a multi-terminal transmission line using synchronized voltage measurements, *IEEE Trans. Power Del*, 20(2), 1325–1331, 2005.
[18] S. Rajendra & P. G. McLaren, Travelling-wave techniques applied to the protection of teed circuits: Multi-phase/multi-circuit system, *IEEE trans. Power App. Syst*, 104(12), 3551–3557, 1985.
[19] A. O. Ibe & B. J. Cory, A travelling wave-based fault locator for two- and three-terminal networks, *IEEE Trans. Power De*l, 1(2), 283–288, 1986.
[20] F. H. Magnago & A. Abur, Fault location using wavelets, *IEEE Trans. Power Del,* 13(4), 1475–1480, 1998.
[21] C. Y. Evrenoso˘glu & A. Abur, Travelling wave based fault location for teed circuits, *IEEE Trans. Power Del,* 20(2), 1115–1121, 2005.
[22] D. Spoor & J. G. Zhu, Improved single-ended traveling-wave fault location algorithm based on experience with conventional substation transducers, *IEEE Trans. Power Del*, 21(3), 1714–1720, 2006.
[23] P. Jafarian & M. Sanaye-Pasand, A traveling-wave-based protection technique using wavelet/PCA analysis, *IEEE Trans. Power Del*, 25(2), 588–599, 2010.
[24] Z. Q. Bo, R. K. Aggarwal, A. T. Johns, H. Y. Li, & Y. H. Song, A new approach to phase selection using fault generated high frequency noise and neural networks, *IEEE Trans. Power Del*, 12(1), 106–115, 1997.
[25] C. Aguilera, E. Orduna, & G. Ratta, Fault detection, classification and faulted phase selection approach based on high-frequency voltage signals applied to a series-compensated line, *Proc. Inst. Elect. Eng.—Gener., Transm. Distrib,* 153, 469–475, 2006.
[26] A. K. Pradhan, A. Routray, S. Pati, & D. K. Pradhan, Wavelet fuzzy combined approach for fault classification of a series-compensated transmission line, *IEEE Trans. Power Del*, 19, pp. 1612–1618, 2004.
[27] A. Ferrero, S. Sangiovanni, & E. Zappitelli, A fuzzy-set approach to fault-type identification in digital relaying, *IEEE Trans. Power Del*, 10(1), 169–175, 1995.
[28] X. Dong, W. Kong, & Tao Cui, Fault Classification and aulted-Phase Selection Based on the Initial Current Traveling Wave, *IEEE Trans. Power Del*, 24(2), 552–559, 2009
[29] J. A. Jiang, C. L. Chuang, Y. C. Wang, C. H. Hung, J. Y. Wang, C. H. Lee, & Y. T. Hsiao, Hybrid framework for fault detection, classification, and location part II: Implementation and test results, *IEEE Trans. Power Del,* 26(3), 1999–2008, 2011.
[30] H. Livani & C. Y. Evrenosoğlu, A Fault Classification and Localization Method for Three-Terminal Circuits Using Machine Learning, *IEEE Trans. Power Del*, 28(4), 2282–2290, 2013.
[31] Z. He, L. Fu, S. Lin, & Z. Bo, Fault detection and classification in EHV transmission line based on wavelet singular entropy, *IEEE Trans. Power Deliv*, 25(4), 2156–2163, 2010.
[32] S. Lin, Z.Y. He, X.P. Li & Q.Q. Qian, Travelling wave time–frequency characteristic-based fault location method for transmission lines, *IET Gener. Transm. Distrib*, 6(8), 764–772, 2012.

Appendix: System data and parameters

Length of total transmission line AB: 400 km
Parameters of transmission line (positive and zero sequences):
Positive sequences: $r_1 = 0.11273\ \Omega$/km $l_1 = 0.9337$ mH/km $c_1 = 12.74$ nF/km
Negative sequences: $r_0 = 0.3864\ \Omega$/km $l_0 = 4.1264$ mH/km $c_1 = 7.751$ nF/km
Sources E_1 and E_2:
Voltage : 500 kV
Positive-sequence impedance: $1.43+j16.21\ \Omega$
Zero-sequence impedance: $3.068+j28.746\ \Omega$
System frequency: 60 Hz